

**Search for  $E_\gamma \geq 5 \cdot 10^{13}$  eV  $\gamma$ -ray transients through  
the BAKSAN and EAS-TOP correlated data**

**BAKSAN and EAS-TOP Collaborations**

*Submitted to Astroparticle Physics*

**INFN – Laboratori Nazionali del Gran Sasso**



## Search for $E_\gamma \geq 5 \cdot 10^{13}$ eV $\gamma$ -ray transients through the BAKSAN and EAS-TOP correlated data

M. Aglietta<sup>a,b</sup>, B. Alessandro<sup>b</sup>, V.V. Alexeenko<sup>c</sup>, Yu.M. Andreev<sup>c</sup>, P. Antonioli<sup>d</sup>, F. Arneodo<sup>e</sup>, L. Bergamasco<sup>b,f</sup>, M. Bertaina<sup>a,b</sup>, C. Castagnoli<sup>a,b</sup>, A. Castellina<sup>a,b</sup>, A. Chiavassa<sup>b,f</sup>, G. Cini Castagnoli<sup>b,f</sup>, B. D’Ettorre Piazzoli<sup>g</sup>, G. Di Sciascio<sup>g</sup>, D.D. Djappuev<sup>c</sup>, W. Fulgione<sup>a,b</sup>, P. Galeotti<sup>b,f</sup>, P.L. Ghia<sup>a,b</sup>, E.N. Gulieva<sup>c</sup>, M. Iacovacci<sup>g</sup>, N.S. Khaerdinov<sup>c</sup>, A.U. Kudzhaev<sup>c</sup>, A.S. Lidvansky<sup>c</sup>, G. Mannocchi<sup>a,b</sup>, O.I. Mikhailova<sup>c</sup>, C. Morello<sup>a,b</sup>, G. Navarra<sup>b,f</sup>, S.Kh. Ozrokov<sup>c</sup>, V.B. Petkov<sup>c</sup>, V.Ya. Poddubny<sup>c</sup>, O. Saavedra<sup>b,f</sup>, G.C. Trincherio<sup>a,b</sup>, Yu.V. Stenkin<sup>c</sup>, V.I. Stepanov<sup>c</sup>, P. Vallania<sup>a,b</sup>, S. Valchierotti<sup>b,f</sup>, S. Vernetto<sup>a,b</sup>, C. Vigorito<sup>a,b</sup>, A.V. Voevodsky<sup>c1</sup>

<sup>a</sup> *Istituto di Cosmo-Geofisica del CNR - Torino - Italy*

<sup>b</sup> *Istituto Nazionale di Fisica Nucleare - Torino - Italy*

<sup>c</sup> *Institute for Nuclear Research, Russian Academy of Sciences - Moscow - Russia*

<sup>d</sup> *Istituto Nazionale di Fisica Nucleare - Bologna - Italy*

<sup>e</sup> *Laboratori Nazionali del Gran Sasso - INFN - Italy*

<sup>f</sup> *Dipartimento di Fisica Generale dell’Università - Torino - Italy*

<sup>g</sup> *Dipartimento di Scienze Fisiche dell’Università and INFN - Napoli - Italy*

### Abstract

A search for transient point sources of ultra-high-energy (UHE)  $\gamma$ -rays has been performed, based on the correlation of two extensive air shower arrays, BAKSAN (North Caucasus, 1700 m a.s.l., BAKSAN Neutrino Observatory, Russia) and EAS-TOP (Campo Imperatore, 2005 a.s.l., Laboratori Nazionali del Gran Sasso, Italy), which are located at very similar latitudes ( $\phi \approx 43^\circ$  N), and separated in longitude

---

<sup>1</sup>deceased

by  $\Delta\lambda \approx 33.7^\circ$ .

The search has been conducted at primary energy  $E_\gamma \geq 5 \cdot 10^{13}$  eV on the timescale of a daily *source* transit over the sky observable in the northern hemisphere ( $19^\circ < \delta < 69^\circ$ ), and for three sources, namely the Crab Nebula, Markarian 421 and Markarian 501, observed at TeV energies by atmospheric Cherenkov detectors.

The stability of the single detectors has been studied and verified up to high significance level.

No coincident excess not compatible with the expectations from statistical fluctuations has been observed. The obtained upper limits to the rate of transient events,  $n_\gamma$ , at 90% c.l., are:

- concerning the sky survey, in the declination band corresponding to the zenith,  $n_\gamma/(\Omega \cdot t) < 12/(\text{yr} \cdot \text{sr})$  with  $\Phi_\gamma(E_\gamma > 5 \cdot 10^{13} \text{ eV}) > 2.0 \cdot 10^{-11} \text{ cm}^{-2} \text{ s}^{-1}$  and duration  $\Delta t < 8$  hrs;
- concerning the candidate sources, e.g., for Markarian 421:  $n_\gamma/t < 7.7/\text{yr}$  with  $\Phi_\gamma(E_\gamma > 5 \cdot 10^{13} \text{ eV}) > 1.3 \cdot 10^{-11} \text{ cm}^{-2} \text{ s}^{-1}$  and  $\Delta t < 7.5$  hrs.

A coincident episode from Markarian 421, observed on January 15th, 1994, with expected chance imitation rate  $n_{ch} = 0.01$  is discussed.

# 1 Introduction

The study of the high energy tail of the spectrum of  $\gamma$ -ray sources is the main tool to investigate the physical processes responsible for the emission and the highest energies reached by the acceleration mechanism of charged particles.

At  $E_\gamma \geq 10^{11}$  eV, direct measurements are still difficult, due to the steepness of the  $\gamma$ -ray spectrum. Such studies are performed by means of ground-based instruments recording the Extensive Air Showers (EAS) produced in the interaction of  $\gamma$ -rays with the Earth's atmosphere: Atmospheric Cherenkov (AC) detectors at energies  $E_\gamma \approx 10^{12}$  eV (VHE) and EAS arrays at  $E_\gamma \approx 10^{14}$  eV (UHE), the main difficulty being due to the charged cosmic ray background.

At VHE, experiments using the AC technique have successfully detected a few  $\gamma$ -ray sources, both galactic, e.g., the Crab Nebula [1, 2, 3, 4, 5] (observed at the same energies also by the Tibet AS- $\gamma$  array [6]) up to  $E_\gamma \approx 5 \cdot 10^{13}$  eV [5], PSR B1706-44 [7, 8], Vela [9], SN1006 [10], and extragalactic, i.e., the Active Galactic Nuclei Markarian 421 [11, 12, 13], Markarian 501 [14, 15, 16, 17], 1ES2344+514 [18]. As at satellite energies, AGNs are characterized by intense sporadic activity superimposing over d.c. fluxes [19, 20, 21].

At UHE, EAS arrays, usually located at mountain altitudes, have set upper limits to d.c. fluxes. At these energies, the most significant effect reported up to now is the outburst observed on February 23, 1989, from the Crab Nebula by the BAKSAN [22], Kolar Gold Field [23] and EAS-TOP [24] arrays. The combined chance imitation rate for the observation is  $3 \cdot 10^{-4}$  and the flux  $\Phi_\gamma(E_\gamma > 2 \cdot 10^{14}$  eV) =  $(2 \pm 1) \cdot 10^{-12}$  cm $^{-2}$  s $^{-1}$ , i.e., about 100 times higher than the extrapolated flux from the ACT data.

Cosmic gamma-ray bursts could also be accompanied by the acceleration of extremely high energy particles [25, 26], and therefore by gamma rays of comparable energy (although with unpredictable time distribution), which would be attenuated by the interactions with the cosmic background photons, while the produced radiation would pile-up at energies  $E_\gamma \leq 10^{14}$  eV.

The search for  $\gamma$ -ray transients at primary energies  $E_\gamma \leq 10^{14}$  eV is thus complementary to the existing gamma-ray astronomies, concerning both known and unknown sources.

From this point of view, EAS arrays, characterized by very high duty cycles and long operation times, can be informative even with respect to AC detectors, in spite of their worse resolution and sensitivity. On the other hand, the establishment of sporadic effects is quite hard with a single detector, due to the cosmic ray background, various sources of noise and the required long exposure times (searches for transient emission using the EAS technique, have been conducted by existing EAS arrays, see e.g. [27, 28, 29]).

We have therefore performed a systematic search for possible coincident excesses in the BAKSAN and EAS-TOP arrays data. The effective energy range of the two experiments is nearly the same due to the similarities of the altitudes and of the individual detectors dimensions and spacings:  $E_\gamma \approx 5 \cdot 10^{13}$  eV, EAS-TOP being more sensitive due to its larger collecting area. Their locations on the Earth (latitudes 43.3° N and 42.5° N, respectively, i.e., very similar, and longitudes 42.7° E and 13.5° E), together with their field of view  $\alpha \approx 40^\circ$ , provide a superposition of about 5 hours for a source culminating at their zenith,

the time shift being  $\Delta t \approx 2$  hours. The coincident experiment, performed on the time basis of a daily source transit, is thus sensitive to transient phenomena, covering the observed time variability range of Markarian 421 and Markarian 501.

The data taking of the two arrays is superimposed for 474 days between 1992 and 1995. The correlated search has been performed over the observable sky ( $19^\circ < \delta < 69^\circ$ ) in cells of dimensions  $4^\circ \times 4^\circ$ , compatible with the angular resolution of both detectors, and for a few candidate sources, namely the Crab Nebula, Markarian 421 and Markarian 501.

## 2 The arrays

### 2.1 The BAKSAN array

The BAKSAN air shower array is located in southern Russia, in the North Caucasus region, near Mount Elbrus (1700 m a.s.l., BAKSAN Neutrino Observatory, lat.  $43.3^\circ$  N, long.  $42.7^\circ$  E).

The array [30] (shown schematically in Fig. 1) consists of a large central scintillator detector (made of 400 liquid scintillator units, total area  $A_C \approx 200$  m<sup>2</sup>) surrounded by 6 smaller ones (each made of 18 units,  $A_s \approx 9$  m<sup>2</sup> each). The array has counting rate  $f \approx 1$  Hz, the trigger being provided by the fourfold coincidence of the detectors nearest to the central one (30 m from the center, indicated as full rectangles in Fig. 1). Only time of flights information are included in the data, so that only the arrival direction can be determined for each shower. For sixfold coincidences (i.e., the ones used in the present analysis) the angular resolution is  $\sigma_\theta \approx 1.5^\circ$ . The typical triggering primary energy in the angular window  $\theta \leq 40^\circ$  is  $E_{typ} \approx 5 \cdot 10^{13}$  eV for a source culminating at the zenith ( $E_{typ}$  being defined as the mode of the distribution  $A(E) \cdot E^{-\gamma}$ , where  $A(E)$  is the array effective area,  $E$  is the primary  $\gamma$ -ray energy,  $\gamma$  is the differential spectrum index, see ref. [31] for further details).

### 2.2 The EAS-TOP array

The EAS-TOP air shower array is located in central Italy, at Campo Imperatore (2005 m a.s.l., National Gran Sasso Laboratories, lat.  $42.5^\circ$  N, long.  $13.5^\circ$  E).

The detector of the electromagnetic component [32] (shown in Fig. 2) consists of 35 scintillator modules 10 m<sup>2</sup> each, spread over an area  $A_{tot} \approx 10^5$  m<sup>2</sup>. Different selection criteria based on the number of fired scintillators and the EAS core location are applied to the data in order to investigate different primary energies. In the present analysis we use (i) showers with  $n_m \geq 4$  fired modules, without core location (Low Energy,  $LE$  events, trigger rate  $f \approx 20$  Hz), and (ii) showers with  $n_m \geq 7$  fired modules and core located inside the edges of the array (High Energy,  $HE$  events, trigger rate  $f \approx 2$  Hz). The angular resolutions are respectively  $\sigma_\theta^{LE} = 2.5^\circ$  (taking into account the uncertainty in core location) and  $\sigma_\theta^{HE} = 0.83^\circ \pm 0.10^\circ$  (obtained through the measurement of the shape of the Moon shadow on the flux of primary cosmic rays [31], thus including systematic

effects). The typical triggering primary energies in the angular window  $\theta \leq 40^\circ$  are  $E_{typ}^{LE} \approx 3 \cdot 10^{13}$  eV and  $E_{typ}^{HE} \approx 9 \cdot 10^{13}$  eV, for a source culminating at the zenith.

### 3 The analysis

The data-set covers the period from 1st January 1992 through 31st December 1995.

#### 3.1 Sky survey

The basis of the sky survey is a daily map in celestial coordinates of the arrival directions of all showers with zenith angle  $\theta_h < 40^\circ$ . The daily maps are produced by tiling the visible sky with a set of approximately equal solid angle cells, whose dimensions are compatible with the angular resolution of both arrays. Cell centers are spaced by  $\Delta\delta = 4^\circ$  in declination, and by  $\Delta\alpha = 4^\circ - 6^\circ - 8^\circ$  in right ascension, depending on  $\delta$ . In order to lessen edge effects, four different series of overlapping maps ( $M_1, M_2, M_3, M_4$ ) are produced, the cells centers being shifted with respect to  $M_1$ : for  $M_2$  by  $(\delta_s = \Delta\delta/2, \alpha_s = 0)$ , for  $M_3$  by  $(\delta_s = 0, \alpha_s = \Delta\alpha/2)$ , for  $M_4$  by  $(\delta_s = \Delta\delta/2, \alpha_s = \Delta\alpha/2)$ . Due to such overlapping, in the most favorable case (a source located in the center of a cell) the angular efficiency  $\epsilon_{ET}^{HE}$  is 0.98 and  $\epsilon_{ET}^{LE} = \epsilon_{BA} = 0.7$ , while in the most unfavorable case  $\epsilon_{ET}^{HE} = 0.7$  and  $\epsilon_{ET}^{LE} = \epsilon_{BA} = 0.5$ . The observed ranges of declination are  $19^\circ < \delta < 67^\circ$  ( $M_1$  and  $M_3$ ) and  $21^\circ < \delta < 69^\circ$  ( $M_2$  and  $M_4$ ), corresponding to 12 declination bands  $\delta_i (i = 1, 12)$ . The number of cells in each band are:

- $\delta_1 \div \delta_4$ :  $\Delta\alpha = 4^\circ \rightarrow 90$  cells
- $\delta_5 \div \delta_8$ :  $\Delta\alpha = 6^\circ \rightarrow 60$  cells
- $\delta_9 \div \delta_{12}$ :  $\Delta\alpha = 8^\circ \rightarrow 45$  cells

for a total of 780 cells for every map.

The search is performed by means of the ON-OFF technique: for each day, every cell is considered a potential  $\gamma$ -ray source (ON) and its number of counts ( $N_{on}$ ) is compared with the number of counts ( $N_{off}$ ) from 6 adjacent cells located in the same declination band and next to the on-source one. For each *source* transit<sup>2</sup>, the significance  $S$  (in units of standard deviations) of the number of observed events is computed according to the Li and Ma statistics [33]:

$$S = \sqrt{2} \left\{ N_{on} \ln \left[ \frac{1 + \alpha}{\alpha} \left( \frac{N_{on}}{N_{on} + N_{off}} \right) \right] + N_{off} \ln \left[ (1 + \alpha) \left( \frac{N_{off}}{N_{on} + N_{off}} \right) \right] \right\}^{1/2} \quad (1)$$

---

<sup>2</sup>A *source* transit is defined as the passage of the considered cell above the chosen *horizon*,  $\theta_h = 40^\circ$ , and the corresponding exposure time,  $T_{exp}$ , is defined as the time between its rising above  $\theta_h$  and setting below  $\theta_h$ .

where  $\alpha = 1/6$ .

For the correlated analysis, days of operation are considered common when overlapping even only partly. As a result of this correlation, 424 BAKSAN daily maps and 474 EAS-TOP ones are used. Maps relative to common days are then searched for statistically significant excesses located in the same position.

## 3.2 Candidate sources search

In the case of known sources the same ON-OFF technique is applied, where the ON cell is centered on the searched source position. For EAS-TOP the cell dimensions are:

$$\Delta\delta = 1.58\sigma_\theta$$

$$\Delta\alpha = \Delta\delta/\cos\delta$$

1.58 being the factor which maximizes the ratio of the signal to the background fluctuations in case of Gaussian angular resolution with r.m.s  $\sigma_\theta$ . For EAS-TOP, in the case of *HE* events  $\Delta\delta = 1.5^\circ$  (the corresponding angular efficiency  $\epsilon_{ET}$  being 0.9), while for *LE* showers  $\Delta\delta = 4^\circ$  ( $\epsilon_{ET} = 0.7$ ). For BAKSAN, the cell dimensions are the same as in the all-sky survey ( $\epsilon_{BA} = 0.7$ ). The six OFF cells are located at the same declination as the source cell (ON) and shifted in right ascension by  $\pm 2K\Delta\alpha$  ( $K = 1, 3$ ). Only events with zenith angle  $\theta_h < 40^\circ$  (which as above defines the *horizon*) are used, and days of operation in which the seven cells are observed without interruptions from their rising above  $\theta_h$  to setting below  $\theta_h$ .

The common data-set includes 356 source daily transits for the Crab Nebula ( $T_{exp} = 5.5$  hrs), 349 for Markarian 421 ( $T_{exp} = 7.5$  hrs) and 360 for Markarian 501 ( $T_{exp} = 7.5$  hrs).

## 4 All-Sky search results

### 4.1 Individual analysis

As a first step of the analysis, the daily maps from each experiment, relative to common days, are studied. The distributions of the daily significances  $S$  are shown in Figs. 3a,b (EAS-TOP, *LE* and *HE* events, respectively,  $780 \times 4 \times 474$  observed cells), and Fig. 3c (BAKSAN,  $780 \times 4 \times 424$  cells). Each of them shows significant negative mean values, which is intrinsic in the usage of Li and Ma statistics and becomes evident in the case of very large number of trials for  $\alpha < 1$  (defined in expr. (1)) [34]: the comparison between the experimental distributions and the simulated ones based on Poissonian fluctuations gives reduced chi-square values  $\chi_\nu^2 = 0.8, 1.1$  and  $1.2$ , for the three cases of Fig. 3, respectively.

The most significant excess is observed in the EAS-TOP *LE* data set ( $S = 5.1$  s.d.). The number of trials being  $N_{tr} = 780 \times 4 \times 474$ , the expected number of such excesses is  $N_{exp} = P(\geq 5.1s.d.) \times N_{tr} = 0.25$ .

The Poissonian behavior of the experimental fluctuations confirms the stability and reliability of both detectors up to the largest observed excesses ( $S \approx 5$  s.d.).



## 4.2 Combined analysis

The absence of statistically significant excesses recorded by a single installation does not preclude the possibility of positive results when combining the two detectors. Such a search on joint data has been conducted with three methods.

- (1) We have searched for possible coincidences, out of statistical expectations, in the upper tails of the daily excesses distributions, sampling at approximately the same significance level  $S$  for both installations. We have selected the  $n_{most}$  largest excesses both in BAKSAN and in the two EAS-TOP data sets:  $n_{most} = 1, 3, 10, 30 \dots$  up to  $N_{most} = 28800$  (corresponding to  $S \approx 2$  s.d.). Among them, coincidences in position and time are searched. The number of measured coincidences,  $C_m$ , is compared with the expected one,  $C_e$ , from chance rate:

$$C_e(n_{most}^{ET}, n_{most}^{BA}) = p(n_{most}^{ET}) \cdot p(n_{most}^{BA}) \cdot N_{trial} \cdot N_{cell} \cdot N_{serie} \quad (2)$$

where:

$$p(n_{most}^{ET}) = \frac{n_{most}^{ET}}{N_{serie} \cdot N_{cell} \cdot N_{days}^{ET}}$$

$$p(n_{most}^{BA}) = \frac{n_{most}^{BA}}{N_{serie} \cdot N_{cell} \cdot N_{days}^{BA}}$$

being:

- $N_{trial} = 675$
- $N_{days}^{ET} = 474$
- $N_{days}^{BA} = 424$
- $N_{serie} = 4$
- $N_{cell} = 780$

where  $N_{trial}$  is larger than both  $N_{days}^{ET}$  and  $N_{days}^{BA}$ , since each daily map from an experiment can overlap with either one or two daily maps from the other one.

$C_e$  and  $C_m$  are compared in Fig. 4 (results for small values of  $n_{most}$ , representing the most significant region for the search of coincidences are given in the table on the same figure): no excess is observed above the chance rate.

- (2) The different sensitivity of the two arrays (due to the larger collecting area of EAS-TOP) has been taken into account by searching for possible coincidences in significance ranges which are not necessarily the same for the two installations. Starting from the individual distributions of daily significances  $S$ , all excesses with  $S > 1.3$  s.d. have been divided into  $N_s$  samples of 1600 each ( $N_s(BA) = 78$ ,  $N_s(ET HE) = N_s(ET LE) = 90$ ), so that  $N_s(BA) \times N_s(ET) = 7020$  cross-correlations are performed. For each combination, the number of expected coincidences is given by expr. (2), with  $n_{most}(ET) = n_{most}(BA) = 1600$ :  $C_e(1600, 1600) = 2.75$ . Figures

5a,b show the distributions of the number of measured coincidences when correlating BAKSAN with EAS-TOP  $LE$  events (Fig. 5a) and with EAS-TOP  $HE$  events (Fig. 5b): the comparison with Poissonian distributions with mean value equal to 2.75 (shown in the same figures) gives reduced chi-square values  $\chi^2_\nu = 0.8$  and 0.5, respectively. No unexpected excess in the number of coincidences is observed for any combination of significance levels.

- (3) In order to take into account the EAS-TOP higher sensitivity, the distribution of the excesses in the BAKSAN data has been studied for the 100 largest EAS-TOP excesses, chosen in the  $LE$  data-set, i.e., at approximately the same primary energy. The resulting distribution is shown in Fig. 6: it is consistent with the expectations from statistical fluctuations. No more significant results are obtained when setting more stringent cuts on EAS-TOP data, i.e., selecting  $n_e < 100$  largest EAS-TOP excesses.

Due to the absence of nonstatistical effects in all procedures, limits to the number of transient emission episodes,  $n_\gamma$ , can be set: e.g., for the declination band corresponding to the zenith, at 90% c.l.,  $n_\gamma < 2.3$  in 474 days of observation with flux<sup>3</sup>  $\Phi_\gamma^{max}(E_\gamma > 5 \cdot 10^{13} \text{ eV}) > 2.0 \cdot 10^{-11} \text{ cm}^{-2} \text{ s}^{-1}$  and duration  $\Delta t < 8 \text{ hrs}$ , i.e.,  $n_\gamma/(\Omega \cdot t) < 12/(\text{yr} \cdot \text{sr})$ , taking into account the dimension and the exposure time of the portion of the declination band above the horizon (in the quoted case  $\Omega = 0.15 \text{ sr}$ ). Values of  $n_\gamma/(\Omega \cdot t)$ ,  $S_{max}$  and  $\Phi_\gamma^{max}$ , for each declination band, are given in Table 1, together with the corresponding  $E_\gamma$  and  $T_{exp}$ .

## 5 Point sources search results

A search for emission from the Crab Nebula, Markarian 421 and Markarian 501 on a daily (single transit) timescale has been conducted in coincidence between the EAS-TOP  $LE$  data set and the BAKSAN one, i.e., at approximately the same primary energy.

---

<sup>3</sup>The flux corresponding to  $n_{obs}$  observed events above primary energy  $E_\gamma$  is given by:

$$\Phi(> E_\gamma) = \frac{n_{obs}}{\int_0^\infty E^{-\gamma} A(E) dE} \frac{1}{\epsilon T_{exp}(\gamma - 1)} E_\gamma^{-\gamma+1} \quad (3)$$

where  $\epsilon$  is the angular efficiency,  $T_{exp}$  is the exposure time,  $\gamma$  is the differential index of the assumed source spectrum and  $A(E)$  is the array effective area as a function of the primary energy  $E$ , calculated through a simulation including both the cascade development in the atmosphere and the detector response. In the present case, we assume  $\gamma = 2$  and we use  $\epsilon = \langle \epsilon \rangle = 0.6$ . Since the exposure time, the primary  $\gamma$ -ray energy and the cell dimensions depend on the declination, fluxes are calculated for each declination band, based on the counting rate of the BAKSAN array (i.e., the less sensitive one) which corresponds to the largest excess detected,  $S_{max}$ .

## 5.1 Individual analysis

The distributions of the daily significances in the individual BAKSAN and EAS-TOP data sets are shown in Figs. 7a,b,c and 8a,b,c for BAKSAN and EAS-TOP, respectively, (Crab Nebula: a, Markarian 421: b, Markarian 501: c). The distributions of Figs. 7,8 are well fitted by zero mean and unit-width Gaussians, as expected (the difference between Gaussian and real behavior is  $\Delta_G \approx 3\%$  in the region around  $S = 3$  s.d.).

## 5.2 Combined analysis

The distributions of correlated BAKSAN and EAS-TOP daily excesses,  $S_{BA}$  and  $S_{ET}$ , for each of the candidate sources, have been studied: fig. 9 shows, as an example, the correlated scatter plot of daily significances in the case of Markarian 421.

Since, as we have shown,  $S_{BA}$  and  $S_{ET}$  follow Gaussian distributions with  $\sigma_{BA} = \sigma_{ET} = 1$ , their combined behavior should follow the Rayleigh distribution:

$$F(R) = \frac{R}{\sigma^2} e^{-\frac{R^2}{2\sigma^2}} \quad (4)$$

where  $R = \sqrt{S_{BA}^2 + S_{ET}^2}$  and  $\sigma = 1$ . From the comparison between the experimental distribution of  $R$  and the expected one, we obtain reduced chi-square values  $\chi_\nu^2 = 0.3, 1.4, 0.8$ , for the Crab Nebula, Markarian 421 and Markarian 501, respectively: the agreement with the expectations from statistical fluctuations is hence quite good.

As a further check, we have studied in the BAKSAN data the distributions of the excesses corresponding to the 10 largest EAS-TOP ones (again to take into account its higher sensitivity). The results are summarized in Table 2: for each distribution (one for each source), mean value and width are given. All distributions and tails are generally consistent with random fluctuations. Limits to the number of bursts of transient emission,  $n_\gamma$ , can then be set, using the maximum excess for each source, as detected by the BAKSAN array, and assuming as differential index for the source spectrum  $\gamma = 2.4$  [35] for the Crab Nebula and  $\gamma = 2$  for the other two sources. At 90% c.l., we have:

- for the Crab Nebula:  $n_\gamma < 2.3$  in 356 daily transits, with  $\Phi_\gamma(E_\gamma > 6 \cdot 10^{13} \text{ eV}) > 1.4 \cdot 10^{-11} \text{ cm}^{-2} \text{ s}^{-1}$  and  $\Delta t < 5.5 \text{ hrs}$ ,  $n_\gamma/t < 10.3/\text{y}$ , taking into account the real daily exposure;
- for Markarian 421:  $n_\gamma < 2.3$  in 349 transits, with  $\Phi_\gamma(E_\gamma > 5 \cdot 10^{13} \text{ eV}) > 1.3 \cdot 10^{-11} \text{ cm}^{-2} \text{ s}^{-1}$  and  $\Delta t < 7.5 \text{ hrs}$ ,  $n_\gamma/t < 7.7/\text{y}$ ;
- for Markarian 501:  $n_\gamma < 2.3$  in 360 transits, with  $\Phi_\gamma(E_\gamma > 5 \cdot 10^{13} \text{ eV}) > 1.4 \cdot 10^{-11} \text{ cm}^{-2} \text{ s}^{-1}$  and  $\Delta t < 7.5 \text{ hrs}$ ,  $n_\gamma/t < 7.5/\text{y}$ .

Slightly peculiar, however, is the case of Markarian 421 for which the mean value of the BAKSAN excesses, corresponding to the 10 largest EAS-TOP ones, is positive at 2.9 s.d. and the second most significant BAKSAN excess ( $S_{BA} = 2.5$  s.d., recorded on 15th January 1994) coincides with the EAS-TOP largest one ( $S_{ET} = 2.6$  s.d.) (this event is

demonstrated in Fig. 9). Following Rayleigh statistics, the number of events expected above the corresponding  $R$  level is 0.6: no nonstatistical significance can thus be inferred from such observation. If we take into account its peculiar location in the uppermost tails of both distributions, we obtain, from the integration of  $F(R)$  for  $S_{ET} > 2.6$  and  $S_{BA} > 2.5$ , an expected chance imitation rate  $n_{ch} = 0.01$ , so that it is worthwhile to point it out.

## 6 Conclusions

A search for possible transient gamma-ray sources (both unpredicted, through a sky-survey of the northern hemisphere, and candidate ones) at  $E_\gamma \geq 5 \cdot 10^{13}$  eV has been performed through the correlation of the BAKSAN and EAS-TOP data. The analysis has been performed on the natural timescale of a daily source transit.

The independent fluctuations of the two arrays counting rates are well understood in terms of Poissonian statistics, up to very large significance values ( $S > 5$  s.d.). This shows that the contributions due to instrumental effects are negligible, and sets a firm base for the further joint analysis.

The correlated data also behave following statistical fluctuations. The absence of non-statistical excesses as a result of the survey over the visible sky ( $19^\circ < \delta < 69^\circ$ ) leads to upper limits to the number of bursts of transient emission,  $n_\gamma$ , (calculated according to the counting rate of the less sensitive array, i.e., BAKSAN). For the declination band corresponding to the zenith, at 90% c.l., we have:  $n_\gamma/(\Omega \cdot t) < 12/(\text{yr} \cdot \text{sr})$ , with flux  $\Phi_\gamma(E_\gamma > 5 \cdot 10^{13} \text{ eV}) > 2.0 \cdot 10^{-11} \text{ cm}^{-2} \text{ s}^{-1}$  and duration  $\Delta t < 8$  hrs ( $n_\gamma$ ,  $\Phi_\gamma$  and  $E_\gamma$  for the different declination bands are given in Table 1).

Three sources, namely the Crab Nebula, Markarian 421 and Markarian 501 (established at TeV energies through the observation of AC detectors) have also been investigated. No significant excesses have been detected from any of them; at 90% c.l., the corresponding obtained upper limits are:

- for the Crab Nebula:  $n_\gamma/t < 10.5/\text{yr}$  with  $\Phi_\gamma(E_\gamma > 6 \cdot 10^{13} \text{ eV}) > 1.4 \cdot 10^{-11} \text{ cm}^{-2} \text{ s}^{-1}$  and  $\Delta t < 5.5$  hrs
- for Markarian 421:  $n_\gamma/t < 7.7/\text{yr}$  with  $\Phi_\gamma(E_\gamma > 5 \cdot 10^{13} \text{ eV}) > 1.3 \cdot 10^{-11} \text{ cm}^{-2} \text{ s}^{-1}$  and  $\Delta t < 7.5$  hrs
- for Markarian 501:  $n_\gamma/t < 7.5/\text{yr}$  with  $\Phi_\gamma(E_\gamma > 5 \cdot 10^{13} \text{ eV}) > 1.4 \cdot 10^{-11} \text{ cm}^{-2} \text{ s}^{-1}$  and  $\Delta t < 7.5$  hrs.

Concerning Mrk421, a marginal effect, observed on January 15th, 1994, with chance imitation rate  $n_{ch} = 0.01$ , if not due to a statistical fluctuation, would prove that the gamma-ray spectrum of AGNs, during flaring activity, extends up to primary energies  $E_\gamma \approx 5 \cdot 10^{13}$  eV (with  $\Phi_\gamma = (1 \div 2) \cdot 10^{-11} \text{ cm}^{-2} \text{ s}^{-1}$ ), with no significant absorption on infrared photons in the intergalactic space at such energies up to the distance of Mrk 421 ( $z=0.031$ ).

**Acknowledgments.** The authors wish to thank the director and the staff of the National Gran Sasso Laboratories for their constant support, as well as C. Barattia, R. Bertoni, G. Giuliani, A. Giuliano and G. Pirali for their technical assistance. Part of this work was supported by INTAS under contract 93-303 and we are indebted to J. Osborne for his precious organization. V.V.A. wishes to thank O.G. Ryazhskaya for kind cooperation and INFN for hospitality.

This work, as well as the whole field of ground based  $\gamma$ -ray astronomy, was initiated thanks to the activity of A.E. Chudakov, to whom we want to express our gratitude.

## References

- [1] T.C. Weekes et al., *Ap. J.*, 342 (1989) 379
- [2] P. Goret et al., *A&A*, 270 (1993) 401
- [3] P. Baillon et al., *Astrop. Phys.*, 1 (1993) 341
- [4] A. Konopelko et al., *Astrop. Phys.*, 4 (1996) 199
- [5] T. Tanimori et al., *Ap. J.*, 492 (1998) L33
- [6] M. Amenomori et al., *Ap. J.*, 525 (1999) L93
- [7] T. Kifune et al., *Ap. J.*, 438 (1995) L91
- [8] P.M. Chadwick et al., *Astrop. Phys.*, 9 (1998) 131
- [9] T. Yoshikoshi et al., *Ap. J.*, 487 (1997) L65
- [10] T. Tanimori et al., *Ap. J.*, 497 (1998) L25
- [11] M. Punch et al., *Nature*, 358 (1992) 477
- [12] D. Petry et al., *A&A*, 311 (1996) L13
- [13] F. Piron et al., *Proc. 26th ICRC, Salt Lake City (USA)*, 3 (1999) 326
- [14] J. Quinn et al., *Ap. J.*, 456 (1996) L83
- [15] S.M. Bradbury et al., *A&A*, 320 (1997) L5
- [16] A. Djannati-Atai et al., *A&A*, 350 (1999) 17
- [17] T. Yamamoto et al., *Astrop. Phys.*, 11 (1999) 141
- [18] M. Catanese et al., *Ap. J.*, 501 (1998) 616
- [19] J.H. Buckley et al., *Ap. J.*, 472 (1996) L9

- [20] M. Catanese et al., *Ap. J.*, 487 (1997) L143
- [21] F. Aharonian et al., *A&A*, 327 (1997) L5
- [22] V.V. Alexeenko et al., *J. Phys. G*, 18 (1992) L83
- [23] B.S. Acharya et al., *Nature*, 347 (1990) 364
- [24] M. Aglietta et al., *Europhys. Letts.*, 15 (1991) 81
- [25] M. Vietri, *Ap. J.*, 453 (1995) 883
- [26] M. Vietri, *Phys. Rev. Letts.*, 78 (1997) 4328
- [27] D.E. Alexandreas et al., *Ap. J.*, 405 (1993) 353
- [28] T.A. Mc Kay et al., *Ap. J.*, 417 (1993) 742
- [29] M. Aglietta et al., *Proc. 1998 Workshop on Frontier Objects in Astrophysics and Particle Physics*, in press
- [30] V.V. Alexeenko et al., *Il Nuovo Cimento*, C10 (1987) 151
- [31] M. Aglietta et al., *Astroparticle Phys.* 3 (1995) 1
- [32] M. Aglietta et al., *Nucl. Instr. and Meth.* A277 (1988) 23; A336 (1993) 310
- [33] Li T.P. and Ma Y.Q., *Ap. J.*, 272 (1983) 317
- [34] Alexeenko V.V. and Ghia P.L., in preparation
- [35] Hillas A.M. et al., *Ap. J.*, 503 (1998) 744

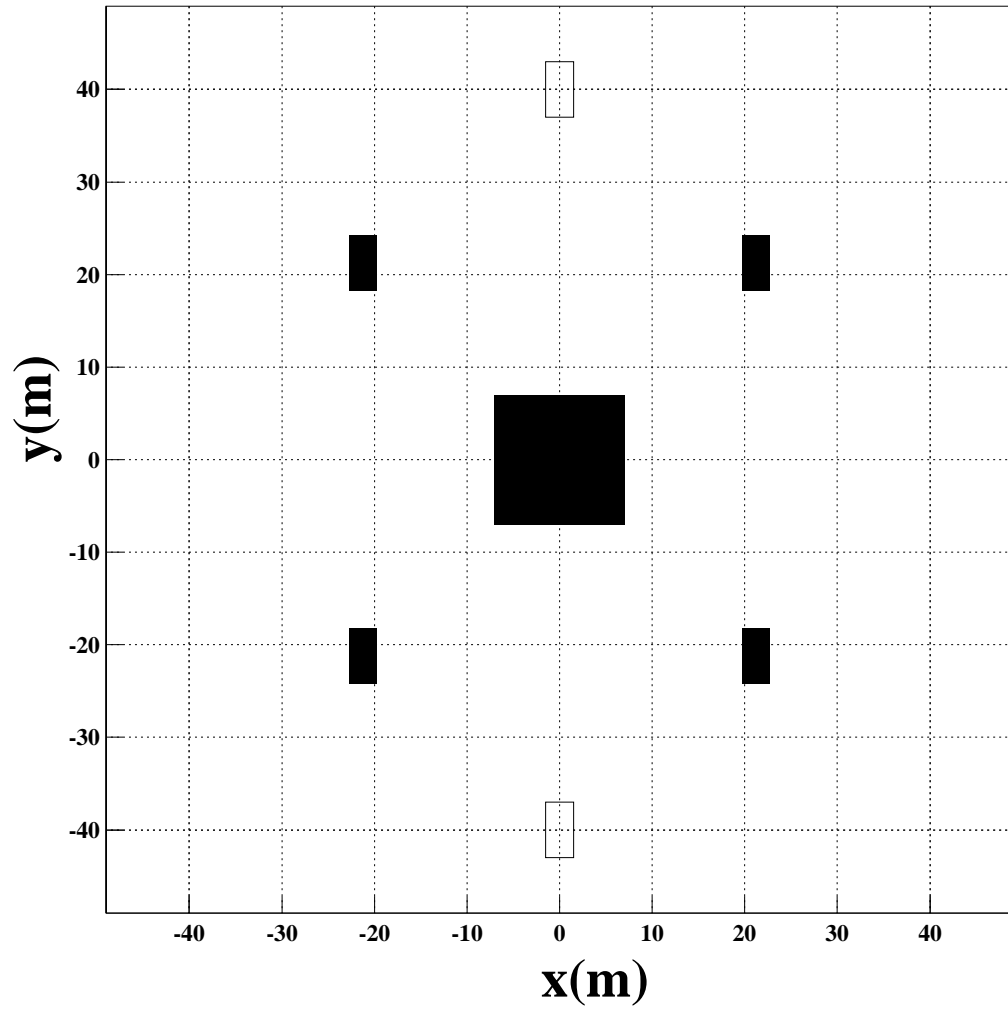


Figure 1: A schematic view of the BAKSAN array

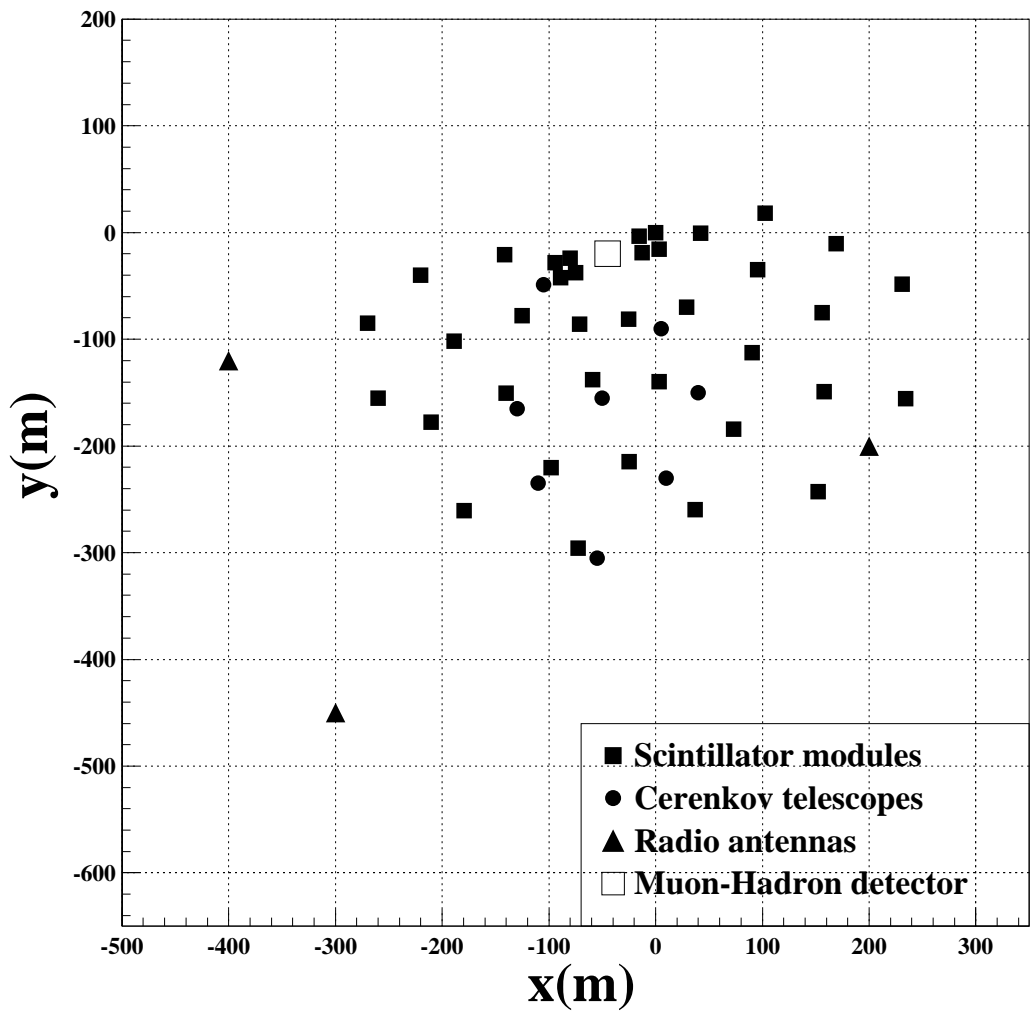


Figure 2: A schematic view of the EAS-TOP array



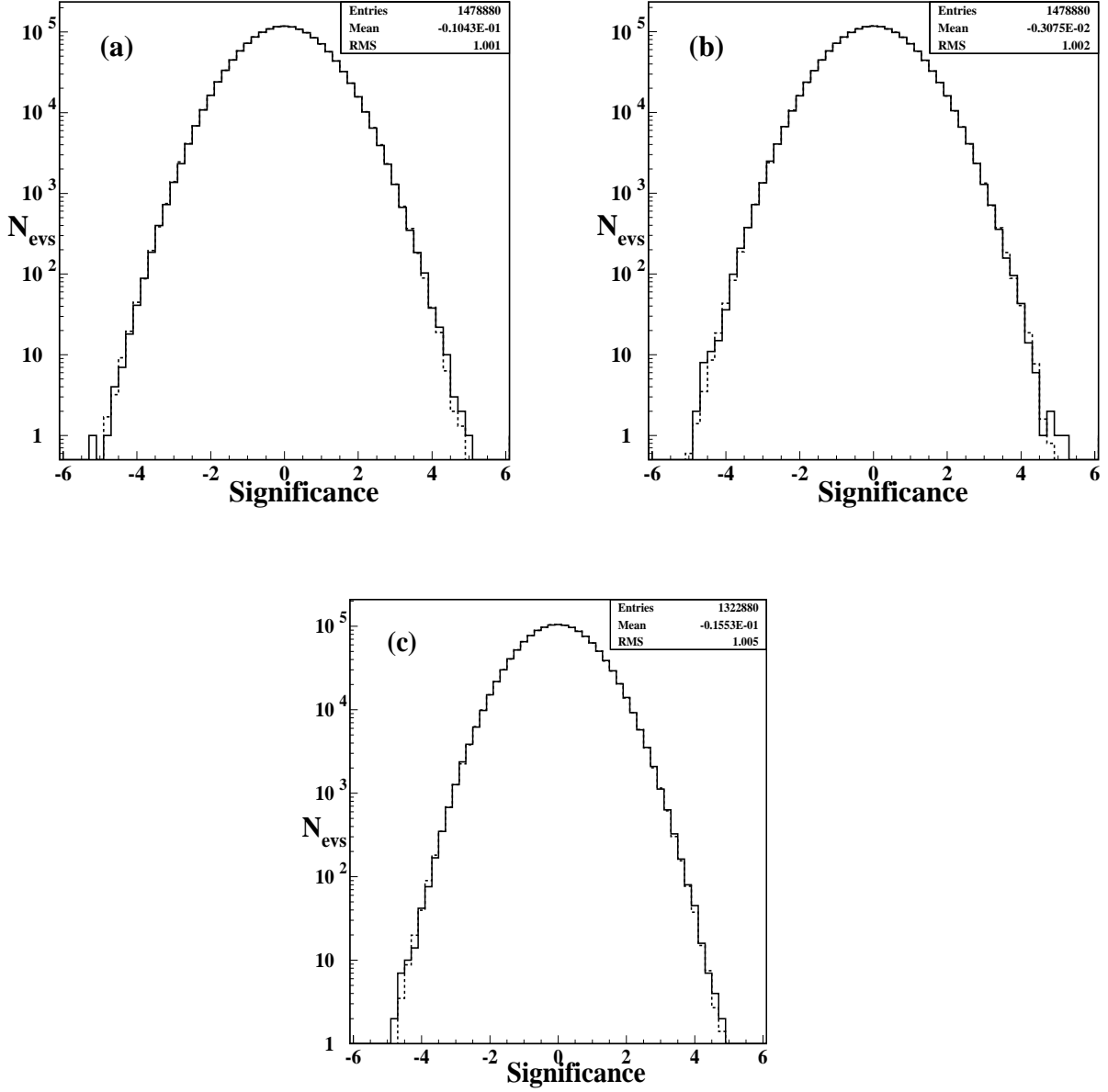


Figure 3: *Distributions of daily significances of the observed excesses in each cell (full lines): (a) EAS-TOP, LE events; (b) EAS-TOP, HE events; (c) BAKSAN. On each experimental distribution, the one obtained from a simulation based on Poissonian fluctuations is shown (dashed line).*

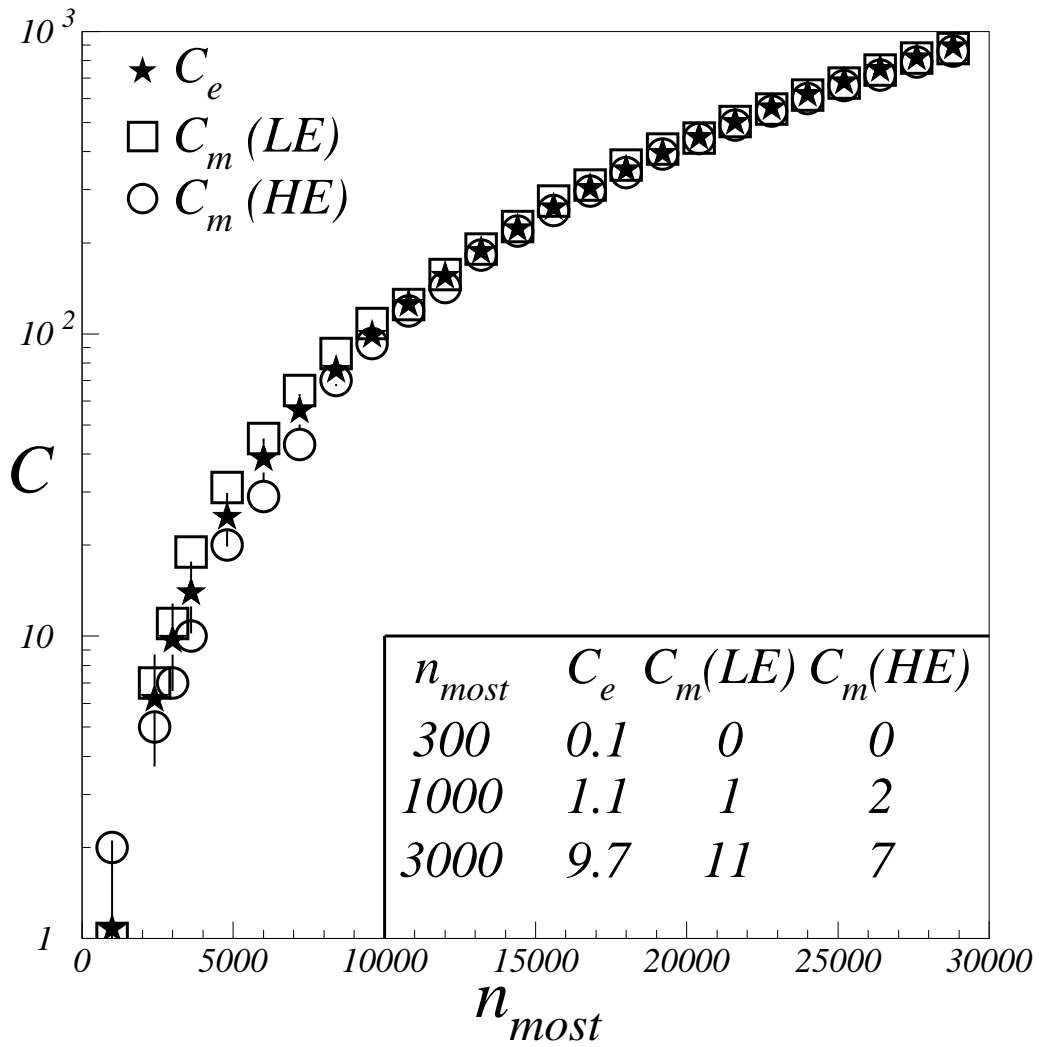


Figure 4: Comparison of measured and expected number of daily coincidences (see text for notation).

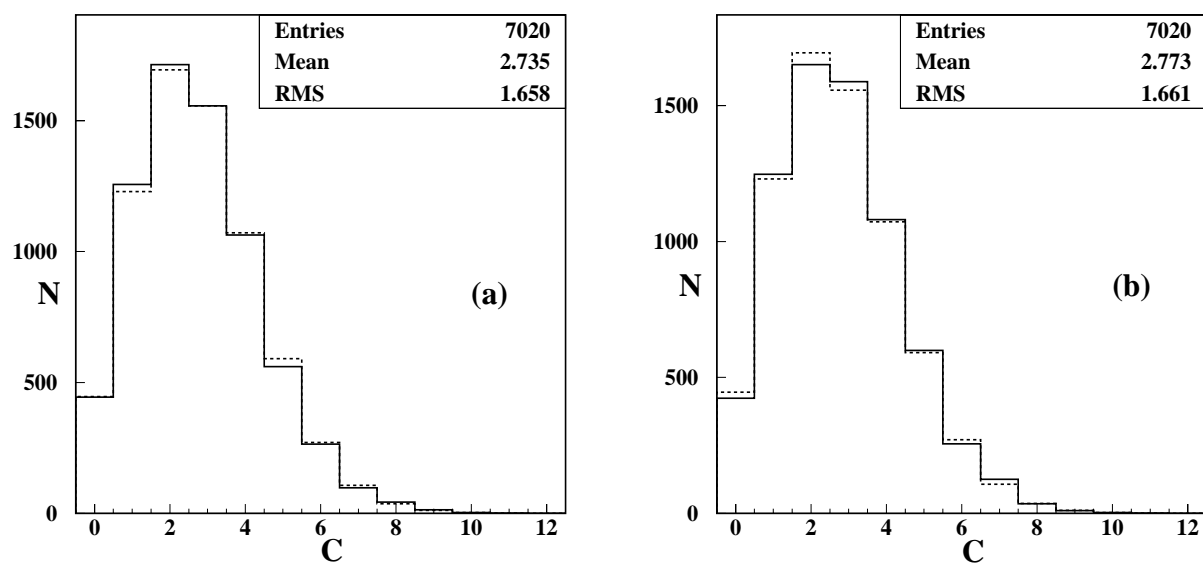


Figure 5: *Distributions of the number of measured coincidences between: (a) BAKSAN and EAS-TOP LE events; (b) BAKSAN and EAS-TOP HE events.*

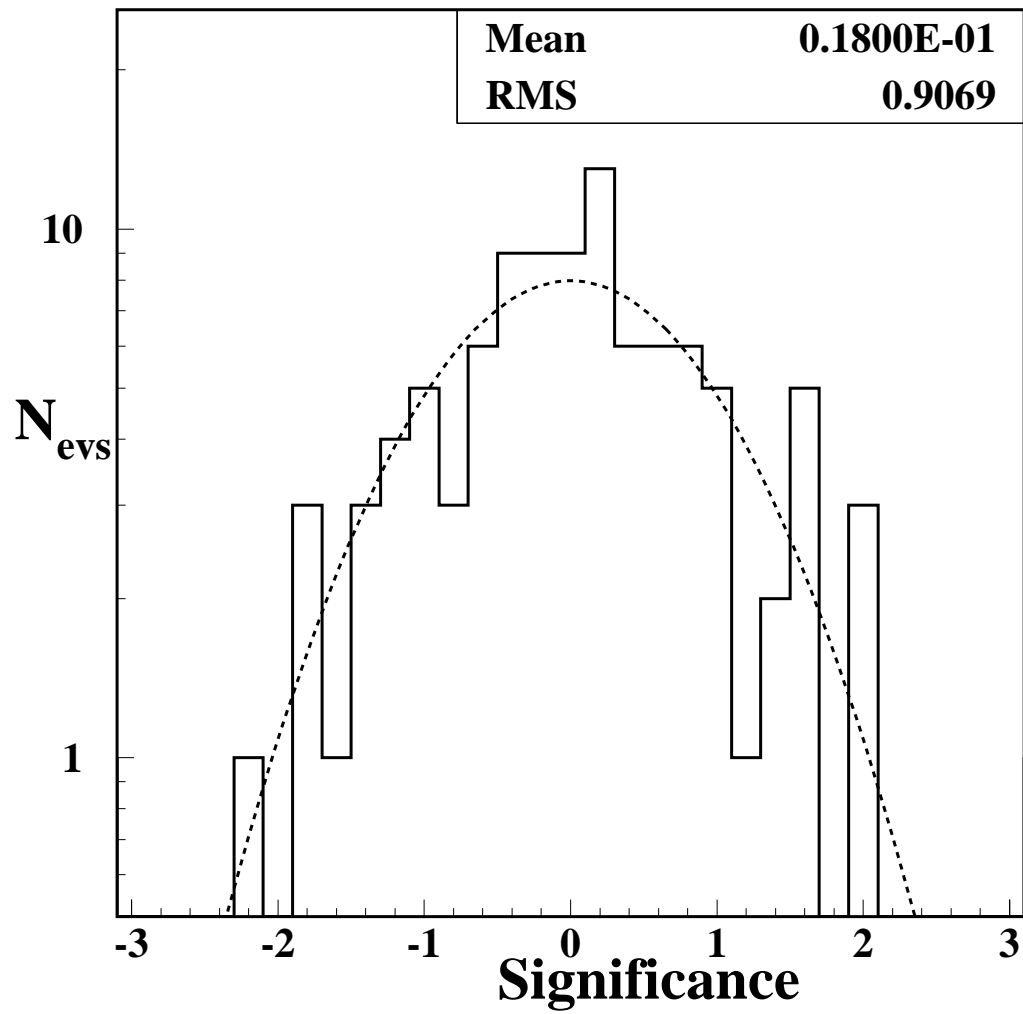


Figure 6: *Distribution of BAKSAN excesses in coincidence with the 100 most significant EAS-TOP LE ones.*

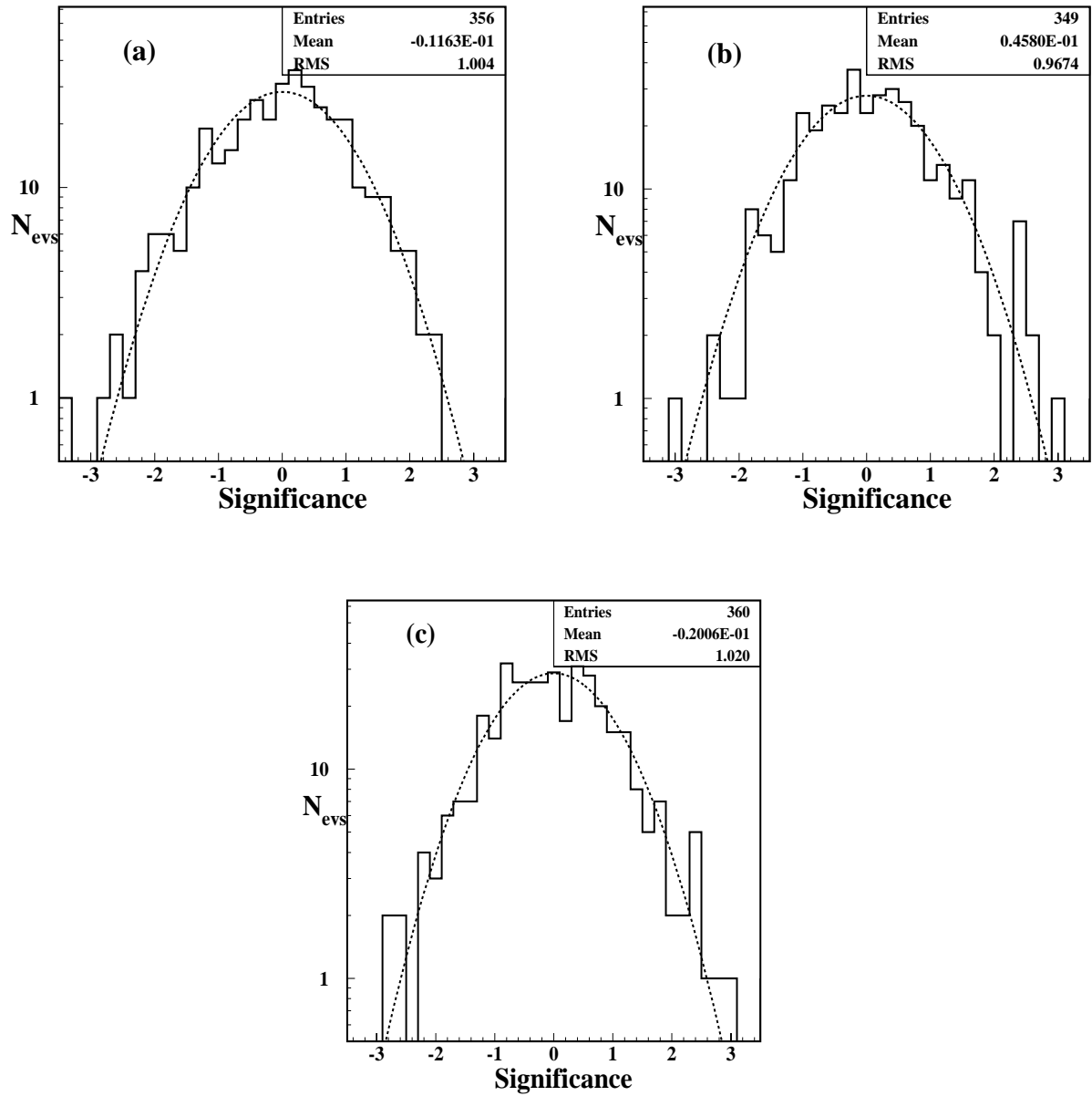


Figure 7: *BAKSAN*: Distributions of daily significances for the three sources Crab Nebula (a), Markarian 421 (b), Markarian 501 (c)

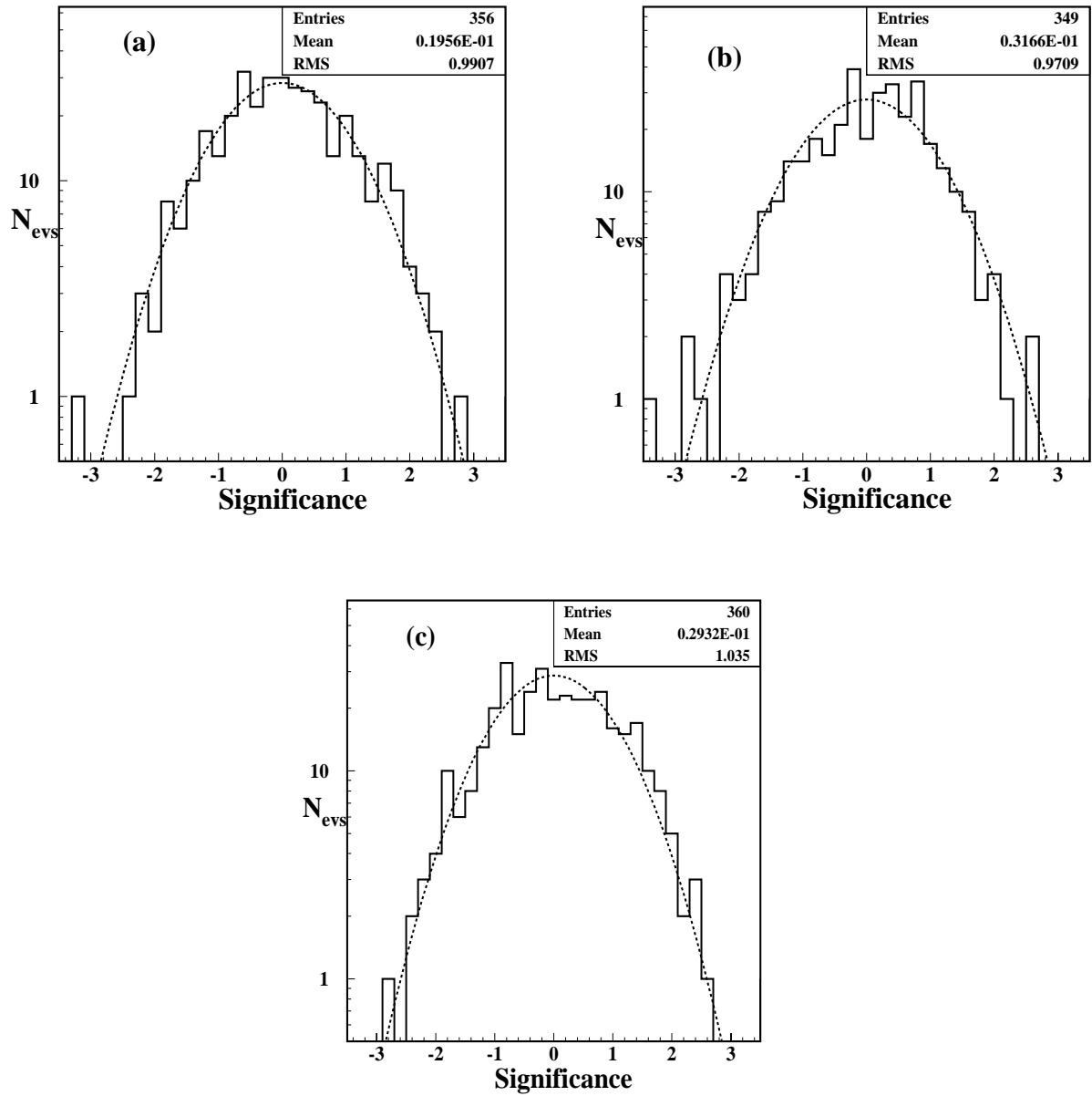


Figure 8: *EAS-TOP*: Distributions of daily significances for the three sources Crab Nebula (a), Markarian 421 (b), Markarian 501 (c)

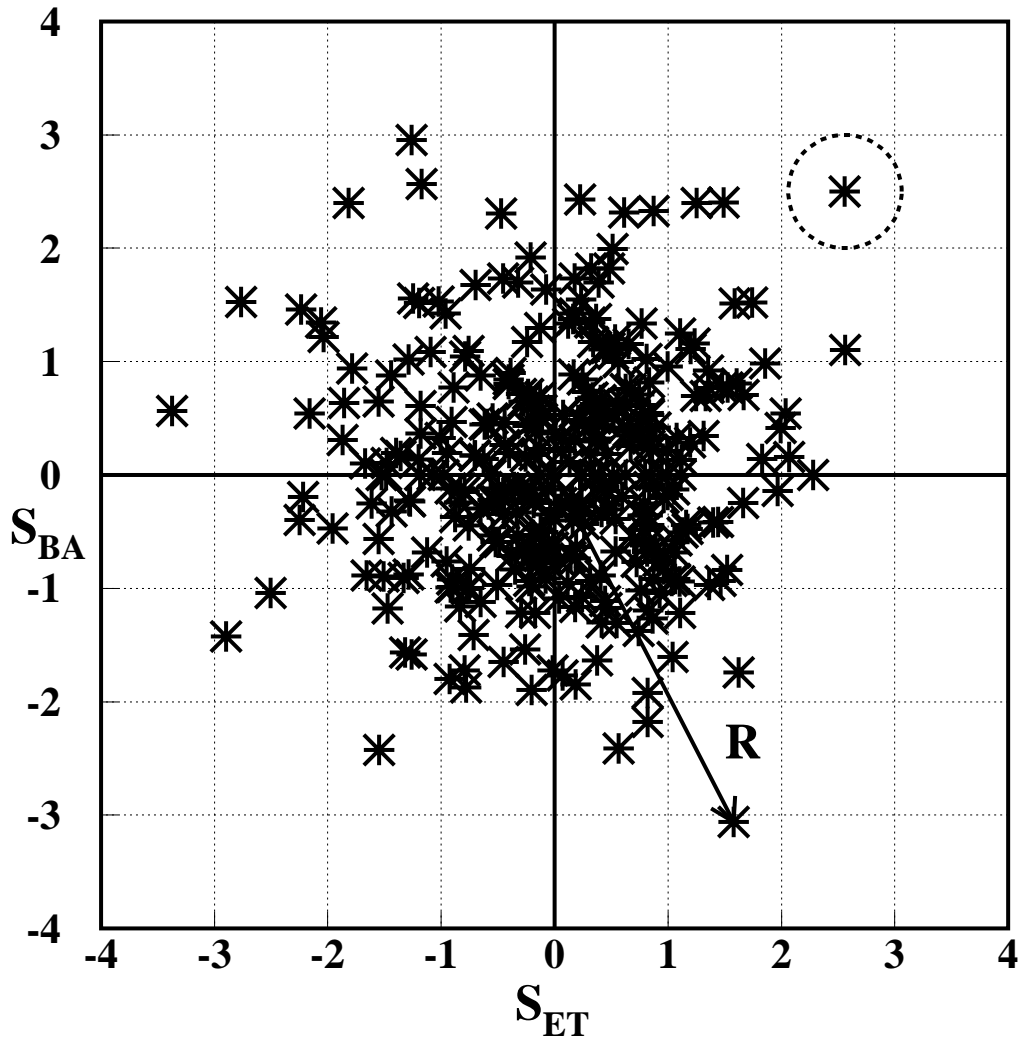


Figure 9: Plot of daily correlated excesses in EAS-TOP ( $S_{ET}$ ) and BAKSAN ( $S_{BA}$ ) in 349 daily transits of Markarian 421. The largest excess discussed in the text is shown.

$\delta$ band	Daily exp. [hrs]	$E_\gamma$ [eV]	$n_\gamma/\Omega \cdot t$	$S_{max}$ [s.d.]	$\Phi_\gamma^{max}$ [ $cm^{-2}s^{-1}$ ]
$\delta_1$	5.5	$8 \cdot 10^{13}$	18.0	4.1	$1.8 \cdot 10^{-11}$
$\delta_2$	6.0	$7 \cdot 10^{13}$	16.4	4.7	$1.9 \cdot 10^{-11}$
$\delta_3$	6.5	$6 \cdot 10^{13}$	15.0	4.4	$1.9 \cdot 10^{-11}$
$\delta_4$	7.0	$5 \cdot 10^{13}$	13.8	4.6	$1.8 \cdot 10^{-11}$
$\delta_5 - \delta_6$	7.5	$5 \cdot 10^{13}$	12.9	4.7	$2.4 \cdot 10^{-11}$
$\delta_7 - \delta_8$	8.0	$5 \cdot 10^{13}$	12.0	4.4	$2.0 \cdot 10^{-11}$
$\delta_9$	8.0	$6 \cdot 10^{13}$	12.0	4.5	$2.2 \cdot 10^{-11}$
$\delta_{10}$	8.0	$7 \cdot 10^{13}$	12.0	4.1	$1.7 \cdot 10^{-11}$
$\delta_{11}$	8.5	$8 \cdot 10^{13}$	11.3	4.4	$1.6 \cdot 10^{-11}$
$\delta_{12}$	8.5	$10 \cdot 10^{13}$	11.3	4.3	$1.3 \cdot 10^{-11}$

Table 1: *Results of the all-sky search: daily exposure, typical primary energy,  $n_\gamma/\Omega \cdot t$  (see text) and the most significant excess detected by the BAKSAN array are given for different  $\delta$  intervals (see sect. 3.1 for the definition of  $\delta_1 - \delta_{12}$ ). Flux upper limits at 90% c.l. are calculated using as average angular efficiency,  $\epsilon=0.6$ , and as differential spectral index,  $\gamma = 2$ , see sect. 4.2.*

Source	Mean value	Width
Crab Nebula	$-0.14 \pm 0.32$	1.0
Mrk 421	$+0.72 \pm 0.25$	0.8
Mrk 501	$-0.27 \pm 0.31$	1.0

Table 2: *Summary of the main parameters of BAKSAN excesses distributions corresponding to the 10 largest EAS-TOP ones, for the Crab Nebula, Markarian 421 and Markarian 501.*